

## Article

# Evaluation of Biocompatibility of 316 L Stainless Steels Coated with TiN, TiCN, and Ti-DLC Films

Jia Lou <sup>1,2</sup> , Beibei Ren <sup>1,2</sup>, Jie Zhang <sup>3,\*</sup>, Hao He <sup>4,\*</sup>, Zonglong Gao <sup>1</sup> and Wei Xu <sup>5</sup>

<sup>1</sup> School of Materials Science and Engineering, Xiangtan University, Xiangtan 411105, China; lou3166@xtu.edu.cn (J.L.); ren3087578860@163.com (B.R.); gaozonglong1996@163.com (Z.G.)

<sup>2</sup> Research and Development Department, Taoyuan Institute of Advanced Manufacturing, Foshan 528000, China

<sup>3</sup> Department of Orthodontics, Changsha Stomatological Hospital, Changsha 410000, China

<sup>4</sup> School of Microelectronics and Materials Engineering, Guangxi University of Science and Technology, Liuzhou 545006, China

<sup>5</sup> The Key Lab of Guangdong for Modern Surface Engineering Technology, National Engineering Laboratory for Modern Materials Surface Engineering Technology, Institute of New Materials, Guangdong Academy of Sciences, Guangzhou 510650, China; xuw0907@163.com

\* Correspondence: kqzj@hnu.edu.cn (J.Z.); 100001865@gxust.edu.cn (H.H.)

**Abstract:** In this study, TiN, TiCN, and Ti-diamond-like carbon (Ti-DLC) films were coated on 316 L stainless steel (AISI 316 L) substrate surface by physical vapor deposition. The biocompatibility of the three films (TiN, TiCN, and Ti-DLC) and three metals (AISI 316 L, Ti, and Cu) was compared on the basis of the differences in the surface morphology, water contact angle measurements, CCK-8 experiment results, and flow cytometry test findings. The biocompatibility of the TiN and TiCN films is similar to that of AISI 316 L, which has good biocompatibility. However, the biocompatibility of the Ti-DLC films is relatively poor, which is mainly due to the inferior hydrophobicity and large amount of sp<sup>2</sup> phases. The presence of TiC nanoclusters on the surface of the Ti-DLC film aggravates the inferior biocompatibility. Compared to the positive Cu control group, the Ti-DLC film had a higher cell proliferation rate and lower cell apoptosis rate. Although the Ti-DLC film inhibited cell survival to a certain extent, it did not show obvious cytotoxicity. TiN and TiCN displayed excellent performance in promoting cell proliferation and reducing cytotoxicity; thus, TiN and TiCN can be considered good orthodontic materials, whereas Ti-DLC films require further improvement.

**Keywords:** Ti-DLC; biocompatibility; wettability; proliferation; apoptosis



**Citation:** Lou, J.; Ren, B.; Zhang, J.; He, H.; Gao, Z.; Xu, W. Evaluation of Biocompatibility of 316 L Stainless Steels Coated with TiN, TiCN, and Ti-DLC Films. *Coatings* **2022**, *12*, 1073. <https://doi.org/10.3390/coatings12081073>

Academic Editor: Alenka Vesel

Received: 4 July 2022

Accepted: 26 July 2022

Published: 29 July 2022

**Publisher's Note:** MDPI stays neutral with regard to jurisdictional claims in published maps and institutional affiliations.



**Copyright:** © 2022 by the authors. Licensee MDPI, Basel, Switzerland. This article is an open access article distributed under the terms and conditions of the Creative Commons Attribution (CC BY) license (<https://creativecommons.org/licenses/by/4.0/>).

## 1. Introduction

AISI 316 L is widely used in medical devices such as orthodontic fixed brackets, because of its excellent machining performance, mechanical properties, corrosion resistance, and cost effectiveness [1,2]. However, when exposed to human oral saliva, AISI 316 L undergoes wear and corrosion, such as crevice corrosion, intergranular corrosion, pitting corrosion, and fretting corrosion [3]. When in contact with human bodily fluids over a long period of time, corroded stainless steel (SS) releases chromium or nickel ions, which induces inflammation and cytotoxic effects [4,5]. At the same time, exposed AISI 316 L releases high concentrations of molybdenum ions, which can pose a threat to human health. Moreover, a larger irregular surface area of exposed SS allows a greater capacity for bacterial adsorption, resulting in poor biocompatibility [6].

To overcome these drawbacks, various coating materials have been applied on the SS surface to reduce application defects and enhance biocompatibility [7]. Such coating materials include TiN, TiCN, and Ti-DLC, which can be applied by physical vapor deposition (PVD), chemical vapor deposition (CVD), and other methods. Due to their simple coating procedure, excellent corrosion resistance, high hardness, and good biocompatibility, TiN films have been widely used in various medical fields such as human implants and surgical

instruments, especially as orthodontic materials [8]. This film not only improves wear resistance and reduces the corrosion rates of the SS substrate, but also inhibits the release of harmful ions. Thus, the biocompatibility of the SS substrate is significantly improved subsequently, enhances the serviceability of the orthodontic part. Subramanian et al. [9] reported that the excellent biocompatibility of TiN/VN multilayer coatings is due to minimal bacterial adhesion on the film surface. Braic et al. [10] analyzed the biocompatibility of TiN and TiN/TiAlN coatings and found that both coatings showed superior biocompatibility to uncoated SS substrates, in terms of cell density, cell viability, and cell morphology. Some researchers have focused on TiCN films, which exhibit higher properties than TiN films; however, their preparation is much more difficult [11]. Ertuerk et al. [12,13] pointed out that as a solid solution of TiN and TiC, TiCN combines the advantages of both materials and exhibits higher hardness, better tribological properties, and better lubrication than TiN in practical applications. In addition, its non-cytotoxic properties combined with its mechanical and corrosive properties make TiCN a very effective material for biomedical applications. Madaoui et al. [14] demonstrated that XC48 steel plated with TiCN in a 3.5% NaCl solution provided better resistance to uniform and pitting corrosion than bare steel, and effectively prevents the release of matrix ions. Antunes et al. [15] reported that compared to uncoated AISI 316 L, TiCN-coated parts exhibited no cytotoxicity or genotoxicity.

Furthermore, DLC films have proven to be potential biomedical materials with excellent performance, due to the fact that DLC has a higher hardness, better wear resistance, and better chemical inertness than TiN and TiCN [16,17]. To overcome the low bonding strength and high internal stress, DLC films are doped with different metals (Cr, Ti, Zr) to reduce the difference in the thermal expansion coefficients between the DLC films and substrates [18,19]. A Ti-DLC film on SS has smaller internal stress, larger film base bonding, and better mechanical properties such as hardness and toughness. In our previous study, Ti-DLC had the lowest surface roughness, while exhibiting high hardness and low COF [20]. Moreover, the Ti-DLC coating exhibits high corrosion resistance because the TiC crystals block the path of corrosive substances through the film [11]. However, a previous study showed that DLC provides a weak cell adhesion matrix when tested with human mesenchymal stem cells, osteoblasts and osteosarcoma cell lines, proving that the compatibility of Ti-DLC films is debatable [21]. Thus, the application of Ti-DLC films on orthodontically fixed brackets still faces significant challenges.

To overcome this limitation, in this study, TiN, TiCN, and Ti-DLC films were coated on the surface of AISI 316 L by using multi-arc ion plating method [11]. Ti, a commonly used dental implant, and Cu, a powerful antimicrobial metal, were used in the experiment for comparison. This study aimed to select a material for coating on AISI 316 L metal implants that would exhibit excellent in-service properties while improving the biocompatibility of AISI 316 L.

## 2. Experimental

In this experiment, AISI 316 L (composition given in Table 1) was used as the substrate material, which was cut into sheets with dimensions of 15 mm × 15 mm × 12 mm. Before depositing, the flaky substrate was sanded with #80-#2000 silicon carbide sandpaper. The sheet substrate was polished to a defect-free mirror finish and cleaned ultrasonically with ethanol for 10 min and deionized water for 5 min to remove surface contamination. The as-treated sheet substrates were placed into an arc coating equipment (Damp AS700, ProChina Limited, Beijing, China) to deposit TiN, TiCN, and Ti-DLC films; the three film deposition parameters were derived from a previous study [20]. The surface morphologies of the deposited films were observed through field emission scanning electron microscopy (SEM, FEI, Nova NanoSEM230, FEI Company, Hillsboro, OR, USA). The contact angle of water on the surface of each sample was measured using a contact angle test system (Orbital surface tension meter, Ramé-hart Model 250, Ramé-hart Instrument Company, Succasunna, NJ, USA) at room temperature (27 °C). The specific test technique used was the solid drop method with a drop volume of 2 µL.

**Table 1.** Composition of AISI 316 L substrate.

Alloy	Main Alloying Elements (wt%)						
- AISI 316 L	Cr 16.30	Ni 14.20	Mo 1.3	N 0.06	C 0.05	Mn 2.03	Fe balance

For this experiment, L929 mouse fibroblasts obtained from the Institute of Advanced Study of Central South University (Changsha, China) were used to explore the biocompatibility of each sample. For cell recovery, frozen tubes containing L929 mouse fibroblasts were placed in a 37 °C water bath and thawed by constant shaking. After an initial observation of L929 mouse fibroblast viability through pressed microscopy, the cells were cultured in modified Eagle's medium (DMEM, Gibco, Life Technologies Corporation, Grand Island, NY, USA) containing 10% fetal bovine serum (FBS). After reaching 80%–90% confluence, the adherent cells were washed, trypsinized, counted, and re-suspended to seed on the samples. Each sample was separately inoculated into a 6-well tissue culture plate. The cellular concentration was  $1 \times 10^4 \text{ mL}^{-1}$  in the medium (DMEM with 10% FBS) and the sample was incubated for 1 week. The culture parameters were as follows:  $(37 \pm 1) \text{ }^\circ\text{C}$  temperature and 5%  $\text{CO}_2$  concentration. The samples were evaluated at 24, 48, and 72 h. The samples containing cells at 24, 48, and 72 h were washed with phosphate-buffered saline (PBS). After cell fixation, dehydration, and drying, the cell adhesion pattern of each sample was observed by SEM at three incubation time points.

All sets of samples from the three time points removed from the culture plate were digested using trypsin and incubated in a 6-well plate for 4 h after adding a CCK-8 reaction solution at 10 mL/well. The absorbance values at 450 nm of the corresponding seven groups of the samples after 24, 48, and 72 h of incubation were measured using an enzyme standardization instrument (ST-360, Dan Ding Shanghai International Trade Co., Ltd., Shanghai, China). Cell proliferation was detected using Cell Counting Kit 8 (CCK-8, Shanghai Beyotime Institute of Biotechnology, Shanghai, China).

Flow cytometry was conducted to detect the rate of apoptosis after staining with Annexin V-FITC/PI Apoptosis Double Staining Kit (bioworld, BD0062-3, Bioworld Technology, Nanjing, China). All samples were digested using trypsin. Cell suspensions were prepared after washing with PBS and placed in flow-through tubes. Annexin V-FITC/PI was then added, and the samples were incubated at 25 °C for 15 min while being protected from light. The apoptosis rate was calculated on the basis of detection by flow cytometry, which was taken as the sum of the percentages of Q2 (late apoptotic cells) and Q3 (early apoptotic cells).

Tests related to biocompatibility must be repeated at least three times to ensure reproducibility. The data obtained from the experiments were statistically analyzed using a relevant software, and the measures conforming to the normal distribution were expressed as  $x \pm s$ . One-way ANOVA was used to compare means between groups, and the least significant difference method was used for two-way comparison. The test level was set at  $p < 0.05$ . Biocompatibility evaluation criteria for relevant in vitro cytotoxicity tests are in accordance with ISO 10993-5.

### 3. Results and Discussions

#### 3.1. Surface Characteristics

The surface morphologies of the films are shown in Figure 1. The surface of the SS substrate was basically smooth and flat, but there were some tiny pores with irregular shapes, which was mainly due to the cutting and polishing effect. After deposition, few pores were observed on the surfaces of the TiN and TiCN films, while some micro-sized TiC particles were observed. The Ti-DLC film exhibited the lowest porosity, but several flaky defects and clusters were observed on its surface. The adhesion of the three films to the substrate is firm [20]. The thicknesses of the TiN, TiCN, and Ti-DLC films were 2.05, 4.10, and 4.48  $\mu\text{m}$ , respectively; further information about the film layer characteristics

and properties can be obtained from previous studies [20]. The SEM images depicting the morphology of the TiC particles of TiCN and Ti-DLC are shown in Figure 2. The TiC particles in the TiCN film were nearly spherical, and their diameters were 1–2  $\mu\text{m}$ ; however, TiC clusters on the Ti-DLC films exhibited irregular shapes. Their diameters were in the sub-micrometer or nanometer range. The number of TiC clusters on the Ti-DLC films was significantly higher than that on the TiCN films.

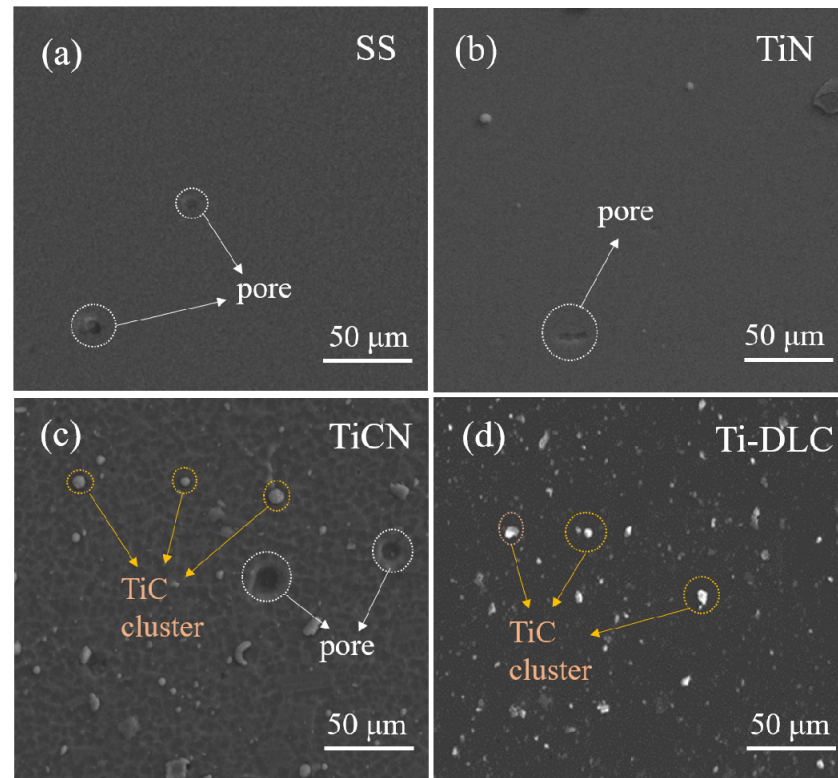


**Figure 1.** SEM images of the surfaces of (a) SS; (b) TiN; (c) TiCN; (d) Ti-DLC.

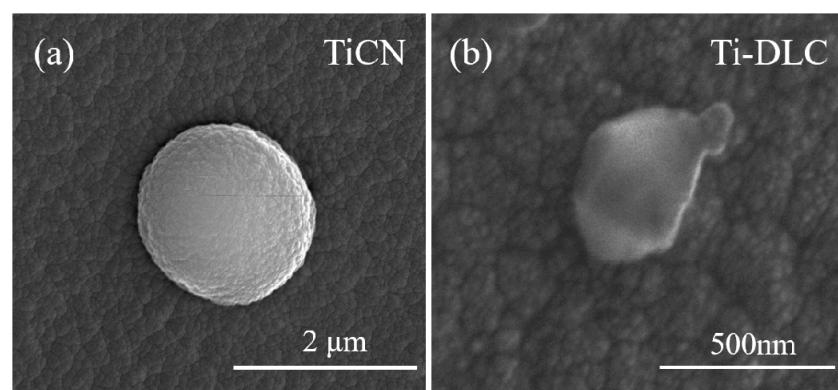


**Figure 2.** SEM images showing the morphology of TiC particles in the films of (a) TiCN and (b) Ti-DLC.

According to our previous results on XRD [20], peaks of C and TiC were observed in both the TiCN and Ti-DLC films, but the latter was more pronounced, indicating that more TiC was formed. From our previous experimental results of Raman spectroscopy [20], the response intensity for  $\text{sp}^2$ -hybridized C in Ti-DLC films was approximately 50 times higher than that for  $\text{sp}^3$ -hybridized C. It was found that a certain amount of  $\text{sp}^3$ -hybridized C was present in the Ti-DLC films, and the D peak area was significantly larger than the G peak

area ( $ID/IG = 2.79$ ). This indicates that the proportion of  $sp^2$ -hybridized C was higher than that of  $sp^3$ -hybridized C.

Figure 3 shows the water contact angle images of all the samples. The water contact angle strongly affects cell adhesion and cell activity [22]. As shown in Figure 3a, SS is hydrophobic, which may be related to its surface porosity and roughness. The TiN and TiCN films substantially improved the wettability of the AISI 316 L substrates. Both films exhibited strong hydrophilicity. Similar results were reported by Khan et al. for TiN [23] and Sunthornpan et al. for TiCN [24]. When AISI 316 L was coated with a Ti-DLC film, the water contact angle increased to  $96.1^\circ \pm 0.4^\circ$  and showed significant hydrophobicity, which is mainly due to the chemical properties of DLC. Graphite and other  $sp^2$  carbon materials are recognized as hydrophobic materials with a water contact angle of  $\sim 90^\circ$ , even when the surface is smooth [25,26]. Some researchers have reported that the surfaces of these materials are susceptible to the adsorption of hydrocarbon contaminants from the air environment [27]. The water contact angle of  $sp^3$ -dominated diamond was slightly lower than that of graphite [28]; however, the proportion of  $sp^2$ -hybridized C in the Ti-DLC films was found to be higher than that of  $sp^3$ -hybridized C. More importantly, the water contact angle of the Ti-DLC film was greater than  $90^\circ$ . This phenomenon can be attributed to the following three factors. (1) The hydrocarbon contaminants in the air cause Ti-DLC to have a larger water contact angle [29]. (2) As Ti-DLC films contain more  $sp^2$  phases and  $sp^2$ -hybridized C have sharp structures on the surface. These sharp structures are arranged in a jagged pattern to give the film layer a large water contact angle. (3) The presence of a large number of TiC nanoclusters with irregular shapes and rough surfaces increased the surface roughness of the Ti-DLC film and thus a large water contact angle.

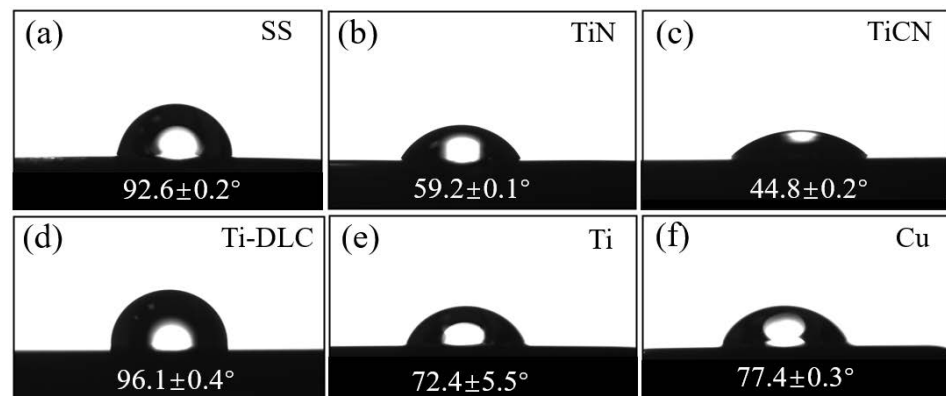


**Figure 3.** Water contact angle of (a) SS; (b) TiN; (c) TiCN; (d) Ti-DLC; (e) Ti; (f) Cu.

### 3.2. Biocompatibility Assay

#### 3.2.1. Cell Adhesion Morphology

Figure 4 shows the morphology of L929 mouse fibroblasts after 24, 48, and 72 h of culture for each sample group. As can be seen from the graph, as the incubation time increased, the blank group exhibited better cell growth morphology than the others. The cells were mainly shuttle-shaped and spread well on the surface of the culture plate. For the 24–72 h culture time, it was found that the number of cells kept on increasing, and the cell spreading status improved with increasing culture time. The L929 cells grew well on the surface of the TiCN and TiN films and SS substrates, among which the cells on TiCN spread maximally on the surfaces of the culture plates. Cell adhesion for the Ti group was slightly weaker than that for the other three film samples. The cells on the Ti-DLC surface had the worst spreading status among those on the three films; this result was similar to that observed for the positive Cu control group. The difficulty in cell adhesion on the Ti-DLC surface is due to its hydrophobicity. More importantly, the Ti-DLC film contains more  $sp^2$  phases, and  $sp^2$ -hybridized C typically has sharper structures on its surface. These sharp structures directly affect the forces between the polar groups of the cellular proteins

and the surface of the material, resulting in weak cell adhesion patterns on the Ti-DLC surface. Although it has rarely been proven that a higher  $sp^2$  ratio negatively affects the cell adhesion of DLC-type coatings, nanodiamond (NCD) and other carbon-based films exhibit similar results. Wang et al. [30] deposited micro-diamond (MCD) and NCD on the surface of a TC4 alloy and found that a higher content of the  $sp^2$  phase in NCD resulted in a lower cell adhesion morphology and reduced cell activity in L929.

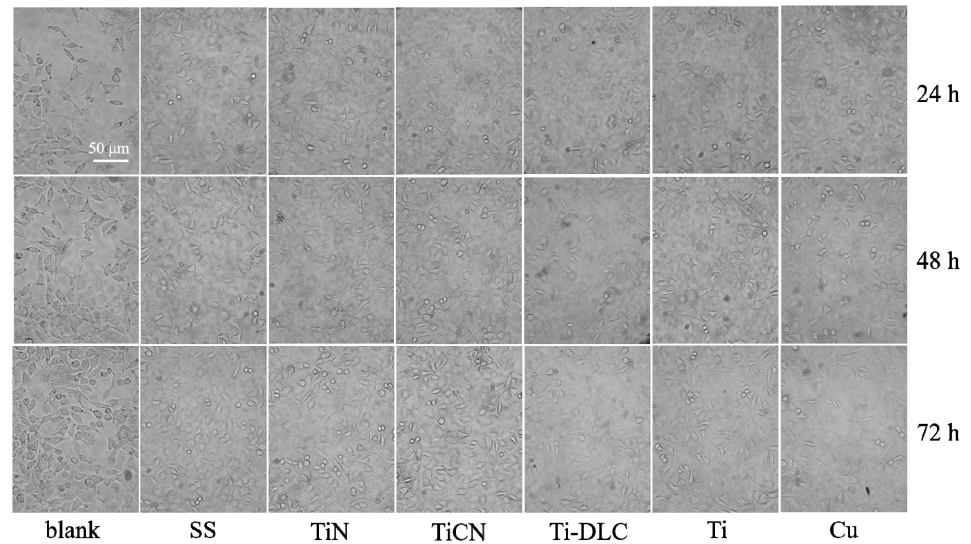


Figure 4. Morphology of L929 cells for the samples after 24, 48, and 72 h of incubation.

3.2.2. CCK-8 Results

Figure 5 shows the absorbance OD values of the culture solution measured at 450 nm for each group at 24, 48, and 72 h of incubation. As shown in Figure 5, the cell counts measured in the SS and TiN groups were similar to those in the blank group for the three studied culture times. The TiN group had the highest number of viable cells and exhibited better biocompatibility than the other groups. The TiCN group had a slightly higher number of cells than the Ti group, especially at 72 h. This indicates that the growth of the cells on the surfaces of SS, TiN, and TiCN was not significantly inhibited and better cell proliferation was demonstrated. The number of cells on the Ti-DLC surface was significantly lower than that on the Ti surface, but much greater than that on the Cu surface.

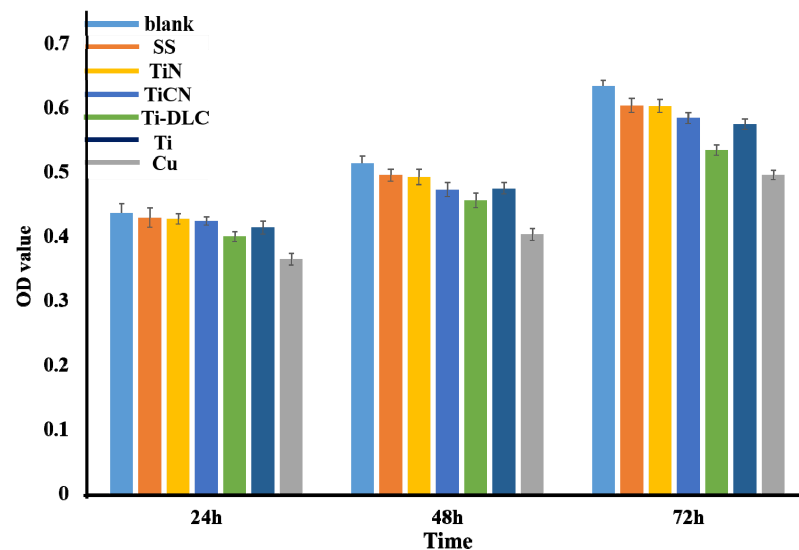


Figure 5. Cell absorbance OD value for the samples after 24, 48, and 72 h of incubation.

The cell proliferation rate is one of the key factors used to determine the biocompatibility of films. Figure 6 shows the relative cell proliferation rate of each sample cultured for 24, 48, and 72 h. Moreover, it is evident from the figure that the cell proliferation rate curves of the SS and TiN groups almost completely overlap. This indicates that there was no difference between the inhibitory effects of SS and TiN on the cells. The cell proliferation rate of the TiCN group was slightly lower than those of the SS and TiN groups. Among the three films, the Ti-DLC group exhibited the lowest cell proliferation rate. The TiN and TiCN groups have higher cell proliferation rates, possibly because they have lower surface roughness and a smaller water contact angle, which is favorable for cell adhesion and growth. The low cell multiplication rate for the Ti-DLC sample was mainly due to its high hydrophobicity. It has been experimentally demonstrated that as the water contact angle increases, the wettability of the material decreases, preventing the cells from attaching to its surface, swelling, and growing well. Eventually, the number of cells, proliferation rates, and differentiation levels are reduced [31].

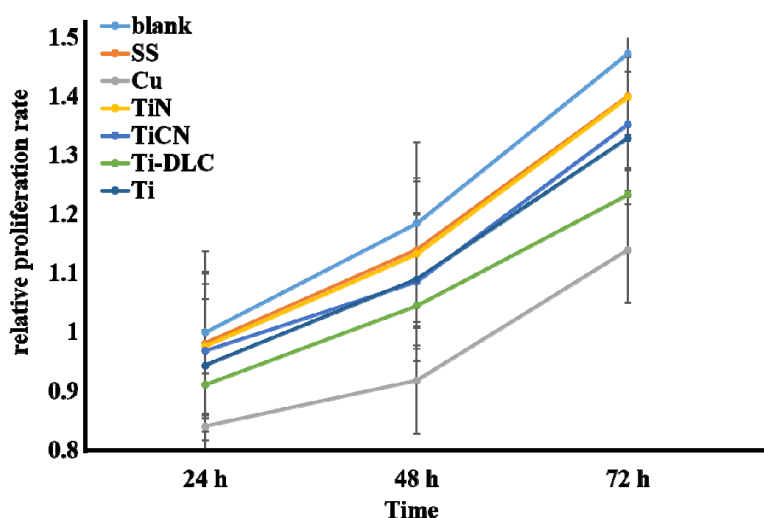


Figure 6. Relative cell proliferation rate for samples after 24, 48, and 72 h of incubation.

### 3.2.3. Flow Cytometry Results

The results of the flow cytometry tests are presented in Table 2. The apoptosis rate was the sum of the Q2 and Q3 quadrant percentages on a two-dimensional scatter plot. Figures 7 and 8, respectively, show the cell flow diagram and total apoptosis rate of each sample at 24, 48, and 72 h of incubation.

Table 2. Flow cytometry test results.

One-Way ANOVA	Mean Diff			Significant		
	24 h	48 h	72 h	24 h	48 h	72 h
Blank vs. SS	-1.52333	-1.79667	-1.71000	0.156N	0.106Y	0.013Y
Blank vs. Cu	-20.30333	-20.80333	-23.36333	0.000Y	0.000Y	0.000Y
Blank vs. TiN	-1.17000	-1.04333	-1.45667	0.380N	0.560Y	0.014Y
Blank vs. TiCN	-0.89	-1.12	-1.73667	0.666N	0.484Y	0.003Y
Blank vs. Ti-DLC	-10.31	-11.87	-12.13	0.000Y	0.000Y	0.000Y
Blank vs. Ti	-5.98	-6.73333	-7.02333	0.000Y	0.000Y	0.000Y
SS vs. Cu	-18.78000	-19.00667	-21.65333	0.000Y	0.000Y	0.000Y
SS vs. TiN	-0.35333	0.75333	0.25333	0.994N	0.873N	0.989Y
SS vs. TiCN	-0.63333	0.67667	-0.02667	0.897N	0.892N	1.000Y
SS vs. Ti-DLC	-8.78667	-10.07333	-10.42000	0.000Y	0.000Y	0.000Y
SS vs. Ti	-4.45667	-4.93667	-5.31333	0.000Y	0.000Y	0.000Y
Cu vs. TiN	19.13333	19.76000	21.90667	0.000Y	0.000Y	0.000Y

Table 2. Cont.

One-Way ANOVA	Mean Diff			Significant		
	24 h	48 h	72 h	24 h	48 h	72 h
Cu vs. TiCN	19.41333	19.68333	21.62667	0.000Y	0.000Y	0.000Y
Cu vs. Ti-DLC	9.99333	8.93333	11.23333	0.000Y	0.000Y	0.000Y
Cu vs. Ti	14.32333	14.07000	16.34000	0.000Y	0.000Y	0.000Y
TiN vs. TiCN	0.28000	−0.07667	−0.28000	0.998N	1.000N	0.982N
TiN vs. Ti-DLC	−9.14000	−10.82667	−10.67333	0.000Y	0.000Y	0.000Y
TiN vs. Ti	−4.81000	−5.69000	−5.56667	0.000Y	0.000Y	0.000Y
TiCN vs. Ti-DLC	−9.42000	−10.75000	−10.39333	0.000Y	0.000Y	0.000Y
TiCN vs. Ti	−5.09000	−5.61333	−5.28667	0.000Y	0.000Y	0.000Y
Ti-DLC vs. Ti	4.33000	5.13667	5.10667	0.000Y	0.000Y	0.000Y

Note: 24 h:  $F = 518.300$ ,  $p < 0.0001$ ; 48 h:  $F = 501.597$ ,  $p < 0.0001$ ; 72 h:  $F = 2103.81$ ,  $p < 0.0001$ .

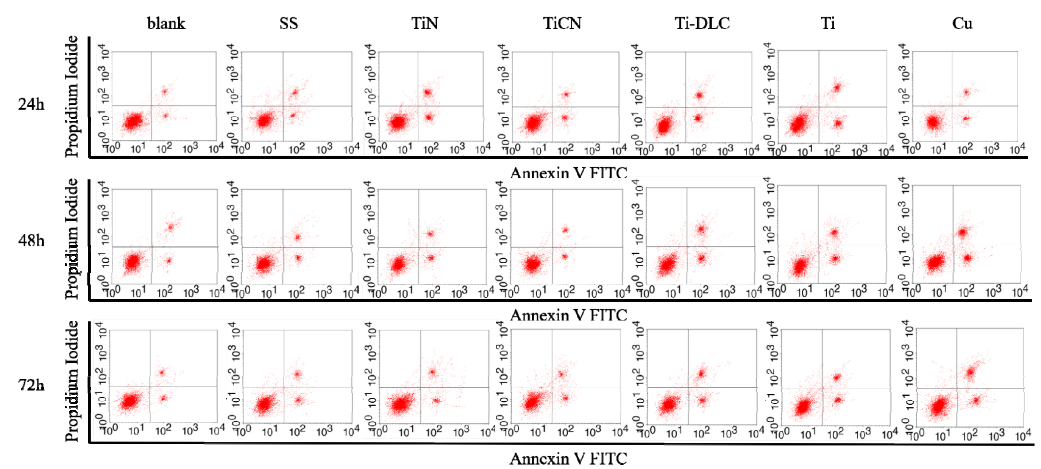


Figure 7. Flow cytometry of samples after 24, 48, and 72 h of incubation.

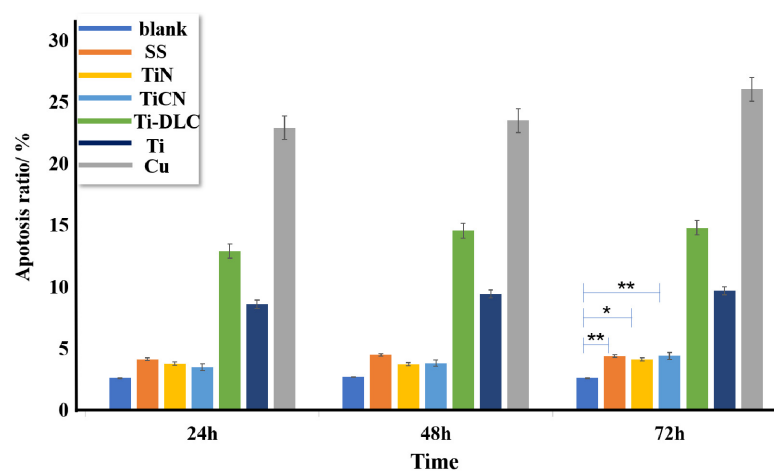


Figure 8. Total apoptosis rate of the samples after 24, 48, and 72 h of incubation.

As can be seen from Figure 8, the blank group had a lower apoptosis rate than the experimental group. The apoptosis rate in the SS group was slightly higher than that in the TiN and TiCN groups but still had a lower apoptosis rate compared to the other experimental groups. This is because the SS surface reacts readily with air to produce a smooth and dense oxide film dominated by oxides of iron and chromium. This film has a certain corrosion resistance, but is still weaker than that of copper and titanium. When placed in harsh environments, such as  $\text{Cl}^-$  and acidic environments, this film is highly susceptible to pitting corrosion over the long term. Corroded SS releases Cr or Ni ions

when present in the oral cavity over time, which in turn causes inflammation and cytotoxic effects [3].

The apoptosis rates of the TiN and TiCN groups were similar at the three time points of 24, 48, and 72 h, and their apoptosis rates were the lowest among the experimental groups. Compared with the apoptosis rate at 24 h, the rate of the TiN film increased by 0.04% at 48 h and 0.69% at 72 h. In contrast, the apoptosis rates of the TiCN films tested at 48 and 72 h increased by 0.32% and 0.63%, respectively. The total apoptosis rate in the SS, TiN, and TiCN groups was less than 5% at all three time points. SS releases harmful ions and thus exhibits a higher rate of apoptosis than TiN and TiCN. TiN has a uniformly dense passivation film and good wettability, which are favorable for cell adhesion and multiplication. As a result, the TiN film exhibited lower apoptosis. Our previous studies have shown that TiC crystals enable TiCN films to exhibit higher corrosion resistance by blocking corrosive substances from penetrating the film path [11]. The high corrosion resistance and hydrophilicity of the TiCN film resulted in the lowest apoptosis rate.

The apoptosis rate in the Ti control group is significantly higher than the three experimental groups mentioned above, and there is a significant difference ( $p < 0.01$ ). Although Ti has a relatively low water contact angle, water contact angle measurements were performed under pure water conditions and short-term action. When Ti is placed in the culture solution for a long time, its passivation film is disrupted and breaks into  $\text{TiO}_2$  particles. This leads to a reduction in the hydrophilicity of the Ti surface, and adhesion decreases due to the continuously increasing surface roughness. McGuff et al. [32] studied histological specimens of septic granuloma and peripheral giant cell granuloma in two patients with peri-implant mucosal enlargement in the oral cavity. They found that broken Ti particles caused these reactive lesions. The highest apoptosis rate was observed in the positive Cu control group. In particular, the total apoptosis rate in the positive Cu control group was as high as  $(26.09 \pm 0.75)\%$  when the cells were cultured for up to 72 h. Cu releases large amounts of Cu ions when it is placed in the culture solution for a long time. High concentrations of Cu ions can cause cellular inhibition and toxicity in humans [33].

The Ti-DLC group had the highest apoptosis rate among the three films, with a total apoptosis rate in the range of 10%–15% at the three time points. The water contact angle of Ti-DLC was  $96.1^\circ \pm 0.4^\circ$ , which indicates hydrophobicity and suggests that it is not conducive to cell reproduction and growth. In contrast, the  $\text{sp}^2$  phase is more abundant in Ti-DLC, and the  $\text{sp}^2$  phases with sharp structures are distributed in a sawtooth shape. By disrupting the cell structure, the Ti-DLC films exhibited more pronounced apoptosis than the other experimental groups [34,35]. Nevertheless, the relevant experimental data show that the cell proliferation rate detected on the surface of the Ti-DLC film at the three culture times was significantly higher than that of the positive Cu control group ( $p < 0.05$ ), while the apoptosis rate was significantly lower than that of the Cu group ( $p < 0.01$ ). This indicates that Ti-DLC does not inhibit cell proliferation or promote apoptosis similar to heavy metals. Moreover, the apoptosis rate of Ti-DLC was only approximately 5% higher than that of Ti at the three culture times. Pure Ti is commonly used for dental implants. Therefore, it is possible to reduce the apoptosis rate of Ti-DLC to that of Ti by improving the preparation process. Thomson et al. [36] assessed cytotoxicity by measuring the activity of  $\beta$ -N-acetyl-D-glucosaminidase in a culture medium of primary peritoneal macrophages from DLC-surfaced mice. The results showed no significant difference in enzyme levels between coated and uncoated pores, and no evidence of cell damage to macrophages on the DLC film surface. It can be concluded that Ti-DLC is not cytotoxic, but less biocompatible than TiN and TiCN films. Our previous studies have shown that Ti-DLC films exhibit the most stable electrochemical properties with excellent corrosion resistance in the presence or absence of artificial saliva and at different concentrations of  $\text{Cl}^-$  and  $\text{H}^+$  [11]. Therefore, Ti-DLC films still hold promise for exploration and development in the biomedical field. The biocompatibility of Ti-DLC can be enhanced by improving the preparation method to reduce hydrophobicity and by enhancing the surface properties or reducing the  $\text{sp}^2$  phase to allow for a better cell attachment state.

#### 4. Conclusions

The biocompatibility of the TiN, TiCN, and Ti-DLC films deposited on AISI 316 L substrates was compared to determine the most suitable bio-coating material for orthodontic dentistry. The main findings of this study are as follows:

- (1) TiN and TiCN had small water contact angles and exhibited significant hydrophilicity. However, Ti-DLC had a relatively large water contact angle and exhibited hydrophobic behavior. The hydrophobicity is mainly due to the large ratio of sp<sup>2</sup> phases. The presence of jagged sp<sup>2</sup> phases and TiC nanoclusters aggravated hydrophobicity.
- (2) TiN exhibited the highest cell value-added rate among the three film samples, followed by TiCN. Ti-DLC exhibited the lowest cell proliferation rate due to its high hydrophobicity and sharp sp<sup>2</sup> phase shape.
- (3) TiN and TiCN films had lower apoptosis rates than SS because of their excellent corrosion resistance. However, the biocompatibility of Ti-DLC is slightly inferior to that of Ti, but significantly better than that of Cu, mainly because of the hydrophobic nature of Ti-DLC. However, Ti-DLC did not exhibit significant cytotoxicity.
- (4) The overall biocompatibility of Ti-DLC was slightly lower than that of the Ti control. Ti-DLC still has potential in the biomedical field, but its preparation must be improved to reduce the amounts of sp<sup>2</sup>-hybridized C and TiC nanoclusters and surface roughness.
- (5) The presence of TiC nanoclusters with irregular shapes increased the surface roughness of the film with TiC. Thus, a large water contact angle is obtained, which is detrimental to cell adhesion and reproduction.

**Author Contributions:** Conceptualization, J.L. and J.Z.; methodology, J.Z.; software, B.R.; validation, J.L., B.R. and H.H.; formal analysis, J.Z.; investigation, J.Z.; resources, W.X.; data curation, B.R.; writing—original draft preparation, B.R.; writing—review and editing, J.L., B.R. and Z.G.; visualization, J.Z.; supervision, H.H.; project administration, J.Z.; funding acquisition, J.L., H.H. and W.X. All authors have read and agreed to the published version of the manuscript.

**Funding:** National Natural Science Foundation of China (52164042). Open project of Foshan Taoyuan Institute of Advanced Manufacturing (TYKF202203004). The Guangdong Academy of Sciences Project of Science and Technology Development (2020GDASYL-20200103109). Guangdong Basic and Applied Basic Research Foundation (2019A1515110710 and 2021A1515012086).

**Institutional Review Board Statement:** Not applicable.

**Informed Consent Statement:** Not applicable.

**Data Availability Statement:** The authors confirm that the data supporting the findings of this study are available within the article.

**Conflicts of Interest:** The authors declare no conflict of interest.

#### References

1. Littlewood, S.J.; Millett, D.T.; Doubleday, B.; Bearn, D.R.; Worthington, H.V. Retention procedures for stabilising tooth position after treatment with orthodontic braces. *Cochrane Database Syst. Rev.* **2016**, *1*, CD002283. [[CrossRef](#)] [[PubMed](#)]
2. Divya, P.; Banswada, S.; Kukunuru, S.; Kavya, K.; Rathod, R.; Polavarapu, K. To compare the accuracy of 0.022 inch slot of stainless steel and ceramic orthodontic brackets marketed by different manufacturers. *J. Pharm. Bioallied Sci.* **2021**, *13*, 1037–1041.
3. Yang, K.; Ren, Y.B. Nickel-free austenitic stainless steels for medical applications. *Sci. Technol. Adv. Mater.* **2010**, *11*, 014105. [[CrossRef](#)] [[PubMed](#)]
4. Xu, X.; Wang, L.; Wang, G.; Jin, Y. The effect of REDV/TiO<sub>2</sub> coating coronary stents on in-stent restenosis and re-endothelialization. *Biomater. Appl.* **2017**, *31*, 911–922. [[CrossRef](#)]
5. Kapnisis, K.K.; Pitsillides, C.M.; Prokopi, M.S.; Lapathitis, G.; Karaiskos, C.; Eleftheriou, P.C.; Brott, B.C.; Anderson, P.G.; Lemons, J.E.; Anayiotos, A.S. In vivo monitoring of the inflammatory response in a stented mouse aorta model. *Biomed. Mater. Res. Part A* **2016**, *104*, 227–238. [[CrossRef](#)] [[PubMed](#)]
6. Kaliaraj, G.S.; Vishwakarma, V.; Kirubakaran, A.M.K. Biocompatible Zirconia-Coated 316 stainless steel with anticorrosive behavior for biomedical application. *Ceram. Int.* **2018**, *44*, 9780–9978. [[CrossRef](#)]
7. Grill, A. Diamond-like carbon coatings as biocompatible materials—an overview. *Diam. Relat. Mater.* **2003**, *12*, 166–170. [[CrossRef](#)]
8. Jun, Z.; Xie, Y.; Zhang, J.; Wei, Q.; Zhou, B.; Luo, J. TiN coated stainless steel bracket: Tribological, corrosion resistance, biocompatibility and mechanical performance. *Surf. Coat. Technol.* **2015**, *277*, 227–233.

9. Subramanian, B.; Ananthakumar, R.; Kobayashi, A.; Jayachandran, M. Surface modification of 316 L stainless steel with magnetron sputtered TiN/VN nanoscale multilayers for bio implant applications. *Mater. Sci. Mater. Med.* **2012**, *23*, 329–338. [[CrossRef](#)] [[PubMed](#)]
10. Braic, M.; Balaceanu, M.; Braic, V.; Vladescu, A.; Pavelescu, G.; Albuлесcu, M. Synthesis and characterization of TiN, TiAlN and TiN/TiAlN biocompatible coatings. *Surf. Coat. Technol.* **2005**, *200*, 1014–1017. [[CrossRef](#)]
11. Lou, J.; Gao, Z.L.; Zhang, J.; He, H.; Wang, X.M. Comparative Investigation on Corrosion Resistance of Stainless Steels Coated with Titanium Nitride, Nitrogen Titanium Carbide and Titanium-Diamond-like Carbon Films. *Coatings* **2021**, *11*, 1543. [[CrossRef](#)]
12. Ertuerk, E.; Knotek, O.; Burgmer, W.; Prengel, H.G.; Heuvel, H.J.; Dederichs, H.G.; Stossel, C. Ti(CN) coatings using the arc process. *Surf. Coat. Technol.* **1991**, *46*, 39. [[CrossRef](#)]
13. Chen, R.; Tu, J.P.; Liu, D.G.; Mai, Y.J.; Gu, C.D. Microstructure, mechanical and tribological properties of TiCN nanocomposite films deposited by DC magnetron sputtering. *Surf. Coat. Technol.* **2011**, *205*, 5228. [[CrossRef](#)]
14. Madaoui, N.; Saoula, N.; Zaid, B.; Saidi, D.; Ahmed, A.S. Structural, mechanical and electrochemical comparison of TiN and TiCN coatings on XC48 steel substrates in NaCl 3.5% water solution. *Appl. Surf. Sci.* **2014**, *312*, 134–138. [[CrossRef](#)]
15. Antunes, R.A.; Rodas, A.C.D.; Lima, N.B.; Higa, O.Z.; Costa, I. Study of the corrosion resistance and in vitro biocompatibility of PVD TiCN-coated AISI 316 L austenitic stainless steel for orthopedic applications. *Surf. Coat. Technol.* **2010**, *205*, 2074–2081. [[CrossRef](#)]
16. Jo, Y.J.; Zhang, T.F.; Son, M.J.; Kim, K.H. Synthesis and electrochemical properties of Ti-doped DLC films by a hybrid PVD/PECVD process. *Appl. Surf. Sci.* **2018**, *433*, 1184–1191. [[CrossRef](#)]
17. Qiang, L.; Zhang, B.; Zhou, Y.; Zhang, J. Improving the internal stress and wear resistance of DLC film by low content Ti doping. *Solid State Sci.* **2013**, *20*, 17–22. [[CrossRef](#)]
18. Li, W.S.; Zhao, Y.T.; He, D.Q.; Song, Q.; Sun, X.W.; Wang, S.C.; Zhai, H.M.; Zheng, W.W.; Robert, J.K. Optimizing mechanical and tribological properties of DLC/Cr<sub>3</sub>C<sub>2</sub>-NiCr duplex coating via tailoring interlayer thickness. *Surf. Coat. Technol.* **2022**, *434*, 128198. [[CrossRef](#)]
19. Wang, D.Y.; Chang, Y.Y.; Chang, C.L. Deposition of diamond-like carbon films containing metal elements on biomedical Ti alloys. *Surf. Coat. Technol.* **2005**, *200*, 2175–2180. [[CrossRef](#)]
20. Zhang, J.; Lou, J.; He, H.; Xie, Y. Comparative investigation on the tribological performances of TiN, TiCN, and Ti-DLC film-coated stainless steel. *JOM* **2019**, *71*, 4872–4879. [[CrossRef](#)]
21. Calzado-Martin, A.; Saldana, L.; Korhonen, H.; Soininen, A.; Kinnari, T.J.; Gomez-Barrena, E.; Tiainen, V.M.; Lappalainen, R.; Munuera, L.; Konttinen, Y.T. Interactions of human bone cells with diamond-like carbon polymer hybrid coatings. *Acta Biomater.* **2010**, *6*, 3325–3338. [[CrossRef](#)] [[PubMed](#)]
22. Peng, F.; Lin, Y.L.; Zhang, D.D.; Ruan, Q.D.; Tang, K.W.; Li, M.; Liu, X.Y.; Paul, K.C.; Zhang, Y. Corrosion Behavior and Biocompatibility of Diamond-like Carbon-Coated Zinc: An In Vitro Study. *ACS Omega* **2021**, *6*, 9843–9851. [[CrossRef](#)] [[PubMed](#)]
23. Khan, S.; Chen, S.N.; Ma, Y.C.; Haq, M.U.; Li, Y.D.; Nisar, M.; Khan, R.; Liu, Y.; Wang, J.X.; Han, G.R. Structural and hydrophilic properties of TiN films prepared by ultrasonic atomization assisted spray method under low temperature. *Surf. Coat. Technol.* **2020**, *393*, 12582. [[CrossRef](#)]
24. Sunthornpan, N.; Watanabe, S.; Moolsradoo, N. Corrosion resistance and cytotoxicity studies of DLC, TiN and TiCN films coated on 316 L stainless steel. *Siam Physics Congress.* **2018**, *1144*, 012013 (SPC2018). [[CrossRef](#)]
25. Adamson, A.W.; Gast, A.P. *The Solid-Liquid Interface- Contact Angle: Experimental Methods and Measurements of Contact Angle*; John Wiley & Sons, Inc.: New York, NY, USA, 1997; pp. 362–372.
26. Raj, R.; Maroo, S.C.; Wang, E.N. Wettability of graphene. *Nano Lett.* **2013**, *13*, 1509–1515. [[CrossRef](#)]
27. Kozbial, A.; Zhou, F.; Li, Z.T.; Liu, H.T.; Li, L. Are Graphitic Surfaces Hydrophobic? *Acc. Chem. Res.* **2016**, *49*, 2765–2773. [[CrossRef](#)] [[PubMed](#)]
28. Chanturia, V.A.; Dvoichenkova, G.P.; Koval'chuk, O.E.; Timofeev, A.S. Surface Composition and Role of Hydrophilic Diamonds in Foam Separation. *J. Min. Sci.* **2015**, *51*, 1235–1241. [[CrossRef](#)]
29. Zhong, B.; Zhang, J.Z.; Wang, H.Q.; Xia, L.; Wang, C.Y.; Zhang, X.D.; Huang, X.X.; Wen, G.W. Fabrication of novel silicon carbide-based nanomaterials with unique hydrophobicity and microwave absorption property. *Int. J. Appl. Ceram. Technol.* **2020**, *17*, 2598–2611. [[CrossRef](#)]
30. Wang, J.; Zhou, J.; Long, H.Y. Tribological, anti-corrosive properties and biocompatibility of the micro and nano-crystalline diamond coated Ti-6Al-4V. *Surf. Coat. Technol.* **2014**, *258*, 1032–1038. [[CrossRef](#)]
31. Feng, F.; Wu, Y.L.; Xin, H.T.; Chen, X.Q.; Guo, Y.Z.; Qin, D.Y.; An, B.L.; Diao, X.O.; Luo, H.W. Surface Characteristics and Biocompatibility of Ultrafine-Grain Ti after Sandblasting and Acid Etching for Dental Implants. *ACS Biomater. Sci. Eng.* **2019**, *5*, 5107–5115. [[CrossRef](#)] [[PubMed](#)]
32. McGuff, H.S.; Heim-Hall, J.; Holsinger, F.C.; Jones, A.A.; O'Dell, D.S.; Hafemeister, A.C. Maxillary osteosarcoma associated with a dental implant: Report of a case and review of the literature regarding implant-related sarcomas. *J. Am. Dent. Assoc.* **2008**, *139*, 1052–1059. [[CrossRef](#)] [[PubMed](#)]
33. Zhang, D.; Ren, L.; Zhang, Y.; Xue, N.; Yang, K.; Zhong, M. Antibacterial activity against *Porphyromonas gingivalis* and biological characteristics of antibacterial stainless steel. *Colloids Surf. B Biointerfaces* **2013**, *105*, 51–57. [[CrossRef](#)] [[PubMed](#)]
34. Nel, A.E.; Madler, L.; Velegol, D.; Xia, T.; Hoek, E.M.; Somasundaran, P.; Klaessig, F.; Castranova, V.; Thompson, M. Understanding biophysico-chemical interactions at the nano-bio interface. *Nat. Mater.* **2009**, *8*, 543–557. [[CrossRef](#)] [[PubMed](#)]

35. Monopoli, M.P.; Walczyk, D.; Campbell, A.; Elia, G.; Lynch, I.; Bombelli, F.B.; Dawson, K.A. Physical–chemical aspects of protein corona: Relevance to in vitro and in vivo biological impacts of nanoparticles. *Am. Chem. Soc.* **2011**, *133*, 2525–2534. [[CrossRef](#)] [[PubMed](#)]
36. Thomson, L.A.; Law, F.C.; Rushton, N.; Franks, J. Biocompatibility of diamond-like carbon coating. *Biomaterials* **1991**, *12*, 37–40. [[CrossRef](#)]